Environ. Sci. Technol. **2003**, *37,* 4052−4059

Delineation of Estuarine Management Areas Using Multivariate Geostatistics: The Case of Sado Estuary

SANDRA CAEIRO,*,† PIERRE GOOVAERTS,‡ MARCO PAINHO,§ AND M. HELENA COSTA||

IMAR, Department of Exact and Technological Sciences of the Portuguese Distance Learning University, R. Escola Politecnica 147, 1269-001 Lisbon, Portugal, Biomedware, Inc., 516 North State Street, Ann Arbor, Michigan 48104-1236, ISEGI/CEGI, Institute for Statistics and Information Management of the New University of Lisbon, 1070-124 Lisbon, Portugal, and IMAR, Faculty of Science and Technology of the New University of Lisbon, 2829-516 Caparica, Portugal

The Sado Estuary is a coastal zone located in the south of Portugal where conflicts between conservation and development exist because of its location near industrialized urban zones and its designation as a natural reserve. The aim of this paper is to evaluate a set of multivariate geostatistical approaches to delineate spatially contiguous regions of sediment structure for Sado Estuary. These areas will be the supporting infrastructure of an environmental management system for this estuary. The boundaries of each homogeneous area were derived from three sediment characterization attributes through three different approaches: (1) cluster analysis of dissimilarity matrix function of geographical separation followed by indicator kriging of the cluster data, (2) discriminant analysis of kriged values of the three sediment attributes, and (3) a combination of methods 1 and 2. Final maximum likelihood classification was integrated into a geographical information system. All methods generated fairly spatially contiguous management areas that reproduce well the environment of the estuary. Map comparison techniques based on κ statistics showed that the resultant three maps are similar, supporting the choice of any of the methods as appropriate for management of the Sado Estuary. However, the results of method 1 seem to be in better agreement with estuary behavior, assessment of contamination sources, and previous work conducted at this site.

Introduction

Coastal areas management is a critical, pressing issue as these ecosystems are among the most endangered and sensitive environments in the world. The coincidence of high natural values and attractiveness for human use has led to conflicts between conservation and development. The Sado Estuary is a good example where these conflicts exist because of its location near industrialized urban zones and its designation as a natural reserve. Therefore, it has become quite inevitable to implement a model of environmental management based on methodologies that enable the evaluation of the Sado Estuary processes (*1*). The delineation of fairly spatially contiguous regions can be very useful to simplify these ecosystems management models.

Spatial heterogeneity is a fundamental environmental characteristic and may therefore be associated with ecological information. The importance of the discontinuities between homogeneous zones for the structure of the ecosystems and the ecosystem dynamics as well as for the maintenance of ecological stability has been well-established (*2*).

The use of boundary overlaps to measure spatial association is preferred to models (such as correlation and regression), which presuppose relationships among variables. Boundaries have inherent scientific interest because their locations reflect underlying biological, physical, and/or social processes. Nevertheless, there is a need for true multivariate techniques where variance/covariance among the variables is explored and the contribution of each variable to the pooled metric is quantified (*3*).

Geostatistical techniques such as kriging allow the estimation of attribute values at unsampled locations taking into account the spatial continuity of the data (*4*). Since kriging is preceded by an analysis of the spatial structure of the data, the averaged spatial variability of the data is already integrated into the estimation/interpolation process (*5*).

Multivariate methods such as principal component analysis (PCA), cluster analysis, and discriminant analysis can be coupled with the different types of kriging (*6*−*8*), allowing one to group sampling sites that both have similar properties and are geographically close. With these multivariate geostatistical techniques, interpolation is improved, small occurrences of one kind of land within others of fairly similar kind are disregarded, and undesirable fragmentation avoided (*7*, *9*). Some of these techniques have been successfully used in soil studies, but few were applied to estuarine environments (*7*, *10*) especially to estimate and map spatially contiguous areas for environmental management purpose.

The main purpose of this paper is to present and compare a set of multivariate geostatistical methodologies to define regions of sediment structure. These regions, described in this work as homogeneous areas, are computed on the basis of the subdivision of continuous sediment physicochemical properties. The technique is illustrated using the example of Sado Estuary management.

Materials and Methods

Study Area. The Sado Estuary is the second largest in Portugal with an area of approximately 24 000 ha. It is located in the West Coast of Portugal, within a boundary box of 8°42′ W, 38°25′ N and 8°57′ W, 38°32′ N. Most of the estuary is classified as a natural reserve but also has an important role in the local and national economy. There are many industries, mainly on the northern margin of the estuary. Furthermore, the harbor-associated activities and the city of Setúbal along with the copper mines on the Sado Watershed use the estuary for waste disposal purposes without suitable treatment. In other areas around the estuary, intensive farming, mostly rice fields, is the main land use together with traditional salt pans and increasingly intensive fish farms (*1*, *11*, *12*).

* Corresponding author phone: (351)213916300; fax: (351)-213969293; e-mail: scaeiro@univ-ab.pt.

† IMAR, Department of Exact and Technological Sciences of the Portuguese Distance Learning University.

‡ Biomedware, Inc.

§ ISEGI/CEGI, Institute for Statistics and Information Management of the New University of Lisbon.

|| IMAR, Faculty of Science and Technology of the New University of Lisbon.

10.1021/es0262075 CCC: $25.00
Published on Web 08/14/2003

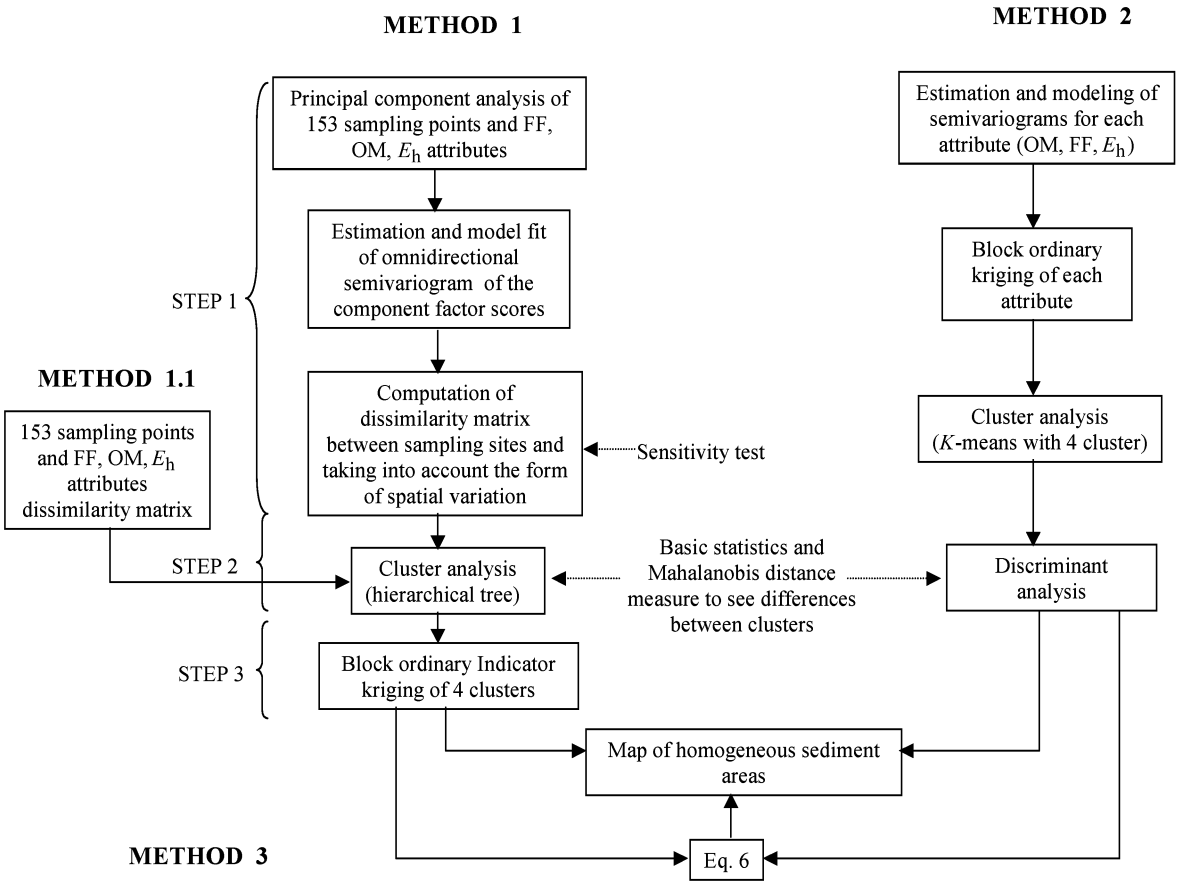

FIGURE 1. Flowchart of the three methodologies used to delineate homogeneous sediment areas.

Sampling Design. From November 2000 to January 2001, sediment samples were collected at 153 sites located using a global positioning system (Garmin GPS 12xL) (*13*). A systematic unaligned sampling design was adopted to provide pairs of close observations required for modeling the short-scale variability as well as a uniform coverage of the area, which tends to reduce the average extrapolation error (*14*). The grid cells are 500 × 750 m, with their length aligned along the direction of azimuth 120°, which corresponds to the water flow and is expected to exhibit less variability (*15*). The grid spacing was based on a preliminary study on the spatial distribution of sediment granulometry, a parameter strongly correlated with sedimentary environment.

Analytical Procedures. At each location, three replicates were taken with a Petit Ponar grab (6 in. Scoopes 00890), and a composite sediment sample was formed. Three attributes, which are strongly related with composition and spatial distribution of benthic organisms as well as contaminant mobility/accumulation, were measured: fine fraction (FF) (%), redox potential (E_h), and total organic matter (OM) (%). This set of sediment attributes integrates the most important properties that characterize the structure and behavior of the sedimentary environment. Also they are easy and fast to measure (*16*, *17*). FF was obtained by hydraulic separation, after organic matter destruction and disaggregation of particles (*18*). Redox potential was measured in situ using an electrode (Hanna Instruments model H 13111). Total organic matter corresponds to the amount lost on ignition at 500 ± 25 °C for 4 h.

Multivariate Geostatistical Analysis. Estuarine management areas were delineated using three different approaches that combine geostatistical prediction and multivariate statistical analysis (see Figure 1):

Method 1. Cluster analysis of dissimilarity matrix that accounts for distances in both the attribute and the geographical spaces, followed by indicator kriging of the classification.

Method 2. Block kriging of the three attributes, followed by a discriminant analysis of K-means clustering predicted values.

Method 3. A hybrid approach that combines the discriminant analysis of method 2 with the indicator kriging used in method 1.

Each approach yields at each unsampled location (100 × 100 m grid), instead of a single class, a vector of probabilities of occurrence of the different categories or clusters. The final classification is obtained by maximum likelihood. Statistical analyses were conducted using Statistica 6.0 software. Semivariograms were built in Variowin 2.2, and kriging was performed using WinGSLIB 1.3.1. The area corresponding to the sampling points was further clipped with the study area boundary including the coast line (*13*) using Arcview/arcinfo 3.2 GIS software.

Method 1. This method, described in Figure 1, starts (step 1) with a PCA of original data (FF, OM, and E_h) followed by computation of experimental semivariograms from the scores of a PCA and fitting of a spherical model. Following ref *6* and with spherical model adjustment (*9*) to take into account the form of spatial variation, the dissimilarity between any two sampling sites i and j is then computed as

$$d_{ij}^* = d_{ij}\frac{c}{c_0 + c}\left[1.5\frac{|u_{ij}|}{a} - 0.5\left(\frac{|u_{ij}|}{a}\right)^3\right] + d_{ij}\frac{c_0}{c_0 + c} \quad \text{for } 0 < u_{ij} \le a$$

$$d_{ij}^* = d_{ij} \quad \text{for } u_{ij} > a \qquad (1)$$

where d_{ij} is the distance in the attribute space between i and j; c is the sill of the spherical semivariogram model; c_0 is the nugget variance; a is the range of the spherical semivariogram model; and u_{ij} is the Euclidean geographic distance between i and j.

The measure d^*_{ij} tends to enhance the dissimilarity between sites that are geographically distant from one another. The use of semivariogram distance, instead of the Euclidian distance, allows one to account for the spatial variability inherent to the study site, in particular the possible existence of anisotropy (i.e., direction-dependent variability). In absence of any spatial correlation, the semivariogram value will be constant for any separation distance (pure nugget effect), and measure d^*_{ij} will identify the distance in the attribute space. The fitting of a model is necessary to be able to derive semivariogram value for all directions and classes of distances, even the ones that have not been sampled. PCA provides an easy way to summarize the information provided by multiple correlated attributes. Oliver and Webster (*6*) and Reed et al. (*7*) found that the semivariogram of the leading principal components explained most of the spatially dependent variation, hence the semivariogram model of the first principal component is used in eq 1.

The Euclidean distance might become inappropriate as a measure of geographical separation if it relates to points over intervening land. Little et al. (*19*) suggested the use of "in-water" distance computed as the length of the shortest in-water path between two sites, which requires contour maps and data layers for GIS analysis. Barabás et al. (*10*) conducted a coordinate transformation prior to analysis, generating a grid within the river that "straightens out" the domain of analysis ensuring that distance are measured within the river. Because the present study is conducted in the estuary bay and not in highly convoluted and short channels, Euclidian distance provides a realistic measure of geographical separation.

In step 2, d^*_{ij} values are assembled into a dissimilarity matrix that undergoes hierarchical clustering using the complete linkage rule (*20*).

In step 3, indicator kriging is used to derive at unsampled locations the probability of occurrence of clusters identified in step 2. The method starts with an indicator coding of classification results $s(\mathbf{x}_\alpha)$ at each sampled location $\mathbf{x}_\alpha$:

$$i(\mathbf{x}_\alpha; s_l) = \left\{\begin{bmatrix}1 \text{ if } s(\mathbf{x}_\alpha) = s_l \\ 0 \text{ otherwise}\end{bmatrix} l = 1, ..., L \right. \quad (2)$$

where L is the number of clusters. For each cluster s_l, experimental indicator semivariograms are then computed and modeled:

$$\gamma(\mathbf{h}; s_l) = \frac{1}{2N(\mathbf{h})} \sum_{\alpha=1}^{N(\mathbf{h})} [i(\mathbf{x}_\alpha; s_l) - i(\mathbf{x}_\alpha + \mathbf{h}; s_l)]^2 \quad (3)$$

Last, the probability of occurrence of the lth cluster at the unsampled location $\mathbf{x}$ is estimated as a linear combination of indicator data:

$$\hat{p}(\mathbf{h}; s_l)|B_{\text{geo}}) = \sum_{\alpha=1}^{N_c} \lambda(\mathbf{x}_\alpha; s_l) i(\mathbf{x}_\alpha; s_l) \quad (4)$$

where B_{geo} is the set of n_c surrounding data $\{s(\mathbf{x}_\alpha), \alpha = 1, ..., n_c\}$. The weights $\lambda(\mathbf{x}_\alpha; s_l)$ are solutions of an indicator kriging system and account for data configuration and spatial continuity of clusters as modeled by indicator semivariograms. Each grid node is assigned to the cluster with the highest probability of occurrence (maximum likelihood classification). Earlier works (e.g., refs *8* and *21*) already demonstrated the usefulness of indicator geostatistics as a methodology for modeling the spatial distribution of categorical variables and estimating probabilities of occurrence of classes based on surrounding observations.

In the end, this method generates relatively smooth maps showing locally dominant classes, uncluttered by outliers. This procedure fulfills the purpose of computing fairly contiguous sediment regions for management and monitoring purposes. To illustrate the benefits of this method, the resulting classification was compared to a map obtained when geographical distances are ignored (see Figure 1 method 1.1, unweighted geographical function).

Method 2. Unlike method 1, this technique first proceeds with the spatial interpolation of environmental attributes, and then a clustering is computed to yield L clusters of sediment structure types. At the end, discriminant analysis is used to compute the cluster classification probabilities at each unsampled location.

It starts with the computation and modeling of the four directional semivariograms of the three attributes (FF, OM, and E_h) (Figure 1). Block ordinary kriging is then performed, yielding at each location $\mathbf{x}$ a vector of $K = 3$ estimated attribute values, $B_z = \{z^*_k(\mathbf{x}), k = 1,..., K\}$, allowing mapping of smooth interpolation surfaces for each attribute.

A K-means clustering of four clusters was then performed on the block kriging entire set. A discriminant analysis is finally conducted with the k-means classification to compute the posterior probabilities of occurrence of each cluster at the unsampled locations. For the discriminant analysis, each unsampled location will fall into one of the L clusters with the same prior probabilities of occurrence ($p_l = 1/L$). A tolerance value of 0.01 was used for each variable. Each grid node is then assigned to the cluster with the highest probability of occurrence, computed as

$$p(\mathbf{x}; s_l|B_z) = \text{Prob}\{S(\mathbf{x}) = s_l|B_z\} = \frac{p_l f(B_z|s_l)}{\sum_{l=1}^{L} p_l f(B_z|s_l)} \quad l = 1, ..., L \quad (5)$$

where p_l is the prior probability of occurrence of class s_l at $\mathbf{x}$ (i.e., $p_l = 1/L$ here) and $f(B_z|s_l)$ is the conditional density of attribute values Z_k given the class s_l. The densities are estimated using a parametric method based on multivariate normal distribution theory. (In this study, the discriminant analysis was used.)

Method 3. The main idea of this hybrid method is to find a way to account for local probabilities of occurrence of each group at unsampled locations, considering the spatial information, into the estimation of $p(\mathbf{x}; s_l|B_z)$ of method 2. A simple approach is based on an equation developed by ref *8* that computes the probability of occurrence of each cluster ($l = 1-L$) by replacing prior probabilities p_l in Bayes' expression (eq 5) by IK-based probabilities (eq 4):

$$p(\mathbf{x}; s_l|B) = \frac{\hat{p}(\mathbf{x}; s_l|B_{\text{geo}}) f(B_z|s_l)}{\sum_{l=1}^{L} \hat{p}(\mathbf{x}; s_l|B_{\text{geo}}) f(B_z|s_l)} \quad l = 1, ..., L \quad (6)$$

where the conditioning data set B includes both attribute (FF, OM, and E_h) and spatial information, $B = B_z \cup B_{\text{geo}}$. This approach amounts to assuming that the prior probability of occurrence of a class s_l is not the same everywhere but depends on the location $\mathbf{x}$. For example, the probability will be large if data belonging to cluster s_l are close geographically. A maximum likelihood classification is then performed on the vector of probabilities. Other works accounting for spatial coordinates (*8*) have shown increases in overall accuracy. In

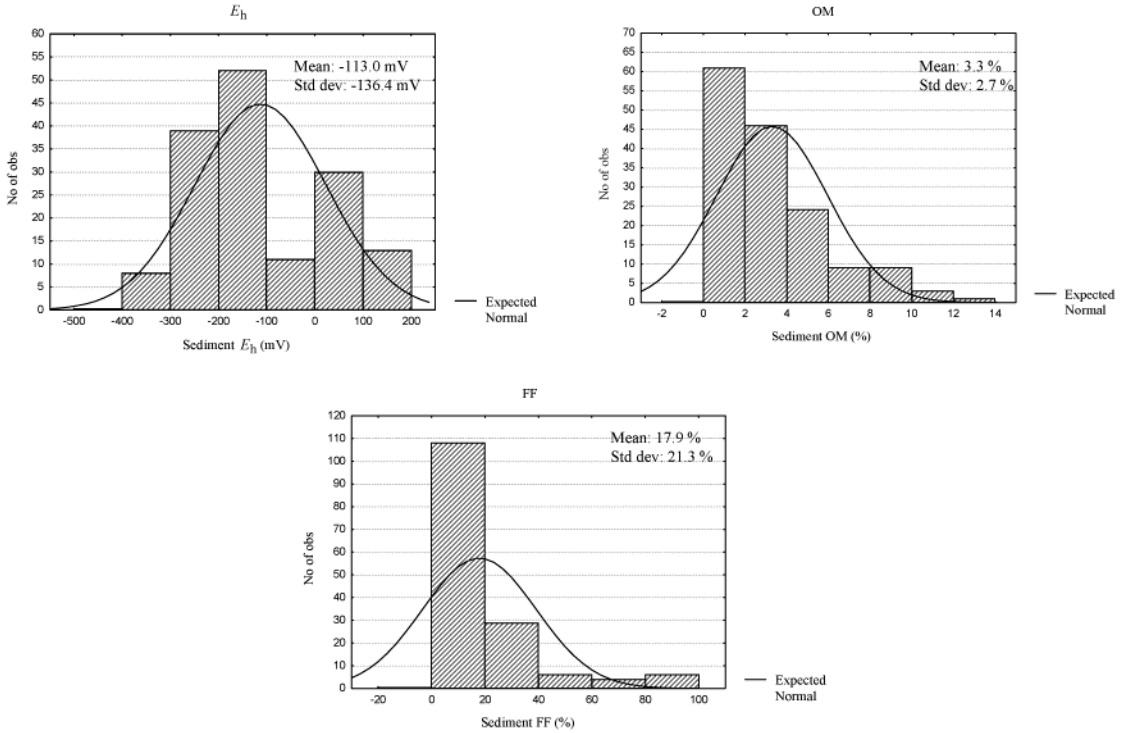

FIGURE 2. Histograms and expected normal distributions of sediment redox potential, organic matter, and fine fraction.

ref *8* and in the present study, the same field data were used to derive the local probabilities of occurrence $\hat{p}(\mathbf{x}; s_l|B_{geo})$ and the functions $f(B_z|s_l)$, although indicator kriging accounts for more information than the discriminant analysis that ignores spatial coordinates. This approach is however purely general, and for example, a training set from another region with similar characteristics could be used to derive the discriminant functions. Similarly the local probabilities of occurrence could be estimated from both field data and secondary information that might not be exhaustively sampled using a multivariate geostatistical approach.

Several statistics to compare the methods were computed, including the κ index of agreement for categorical data. This statistic was adopted by the remote sensing community to assess map similarity and was computed following Cohen (*22*).

Results and Discussion

Distributions of FF and OM are positively skewed, and natural logarithms were applied to make the distribution more symmetric and to stabilize the variance (Figure 2 and in Supporting Information Table A1). E_h needed no transformation. The three variables are moderately correlated, suggesting that PCA would allow one to summarize this information.

In method 1, PCA was performed on the variance−covariance matrix of the three attributes, leading to a first principal component explaining 88% of the total variance. Figure 3 shows the corresponding semivariogram with the model fitted, which will be used for the computation of dissimilarity measures d^*_{ij} (eq 1). The hierarchical classification yielded four clusters that are reasonably distinct with a decline in organic load from cluster 1 to cluster 4, confirmed by an increase of the Mahalanobis distance between these clusters (Table 1 and Supporting Information Table A2). For each cluster, the indicator semivariogram was computed along four directions (Figure 4 and Supporting Information Table A3), and a geometric anisotropy model was fitted visually. All semivariograms display longer ranges in the direction of azimuth 120°, which corresponds to the

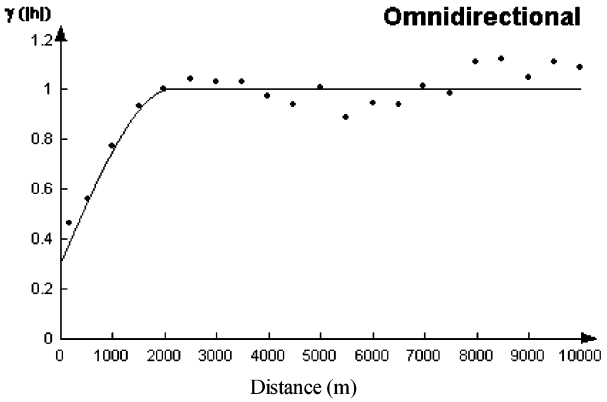

FIGURE 3. Experimental semivariogram of the first principal component with the spherical model fitted. $c_0 = 0.31$, $a = 2159$ m, and $c = 0.7$.

water flow and is in agreement with other studies (*15*). Figure 5 (methods 1 and 1.1 on the left-hand side) shows the results of the maximum likelihood classification performed on estimated probabilities, weighting and unweighting the geographical function. Clusters computed with the weighted geographical function show reasonable spatial continuity with, for a separation distance of up to 400 m, 50% of locations belonging to the same cluster. This proportion is only 30% if the cluster analysis is based on the dissimilarity measure d_{ij}, which ignores spatial coordinates of observations, instead of d^*_{ij} (following the Goovaerts and Webster (*23*) procedure; see Supporting Information). This hierarchical classification based on d_{ij} also yielded a small cluster (cluster 3) of only four locations, distant from each other. It is not possible to classify this cluster due to the high standard deviations of the attribute concentrations (see Table 1 and Figure 5, undefined group in method 1.1). This unweighted classification apparently created a reduced number of areas since it classifies the major part of the estuary as medium high organic load (65%, due to a large area occupying 36 km^2 of the estuary; see Table 1) followed by low organic load classification (23%).

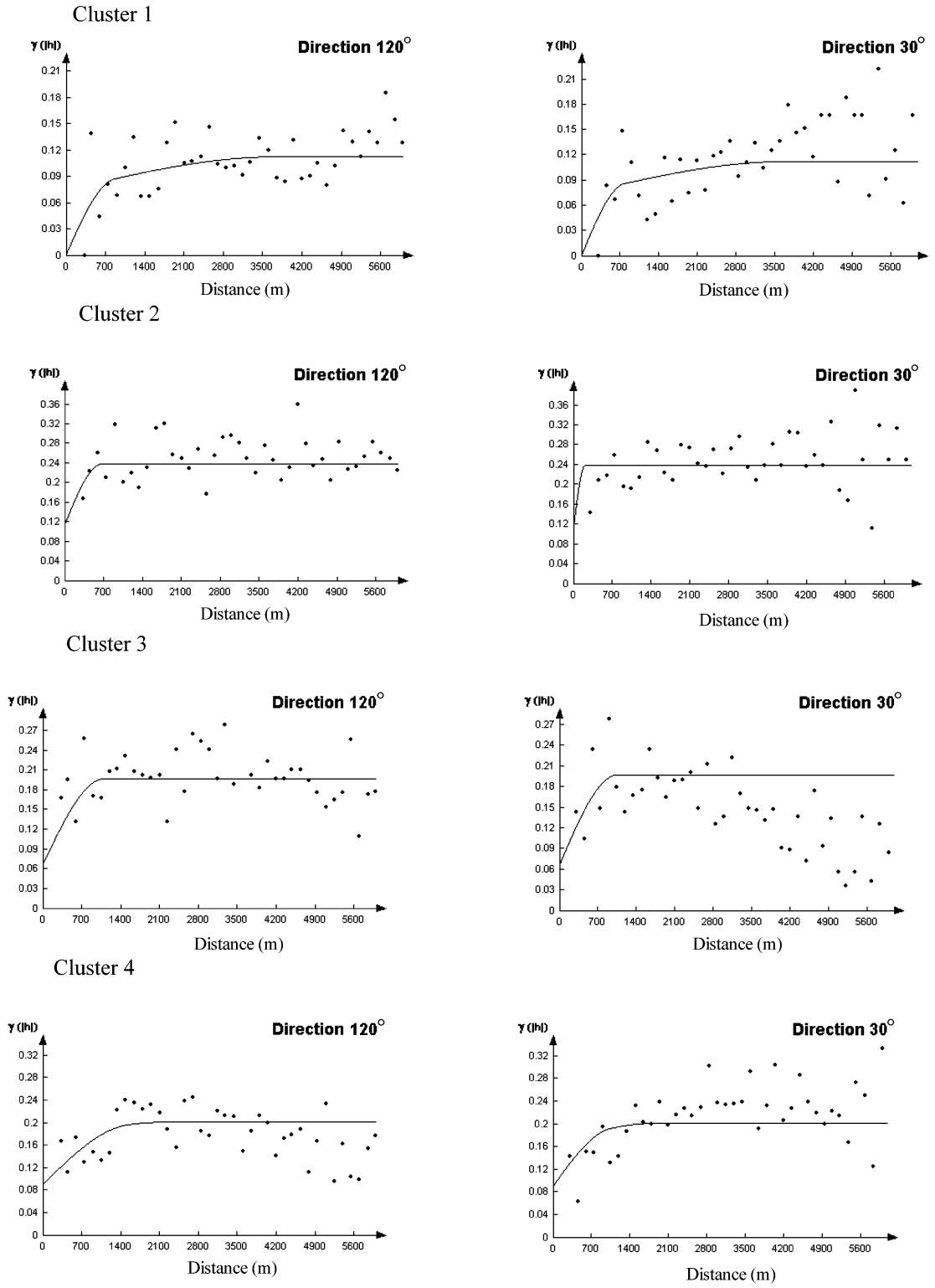

FIGURE 4. Experimental directional semivariograms of cluster data with the model fitted for 120°, the major direction of anisotropy, and the perpendicular direction (30°).

This classification does not reproduce the estuary behavior as explained further in this work. Also it creates a high percentage of areas smaller than the grid cell size (≤0.375 km^2) (74% of the total number of areas). All these reasons support the use of multivariate geostatistics in method 1 as a tool for delineation of estuarine management areas. Method 1.1 was thus discarded for further use.

Method 2 started with the computation of experimental semivariograms for each attribute (FF, OM, and E_h) and the fitting of an anisotropic model (Figure 6 and Supporting Information Table A4). The discriminant analysis with the calibration of four *K*-mean cluster-predicted values yielded a total of 97,5% correctly classified locations. The organic load in the discriminated clusters decrease from cluster 1 to cluster 4, as illustrated by an increase in the Mahalanobis distance between them (Table 1 and Supporting Information Table A5). The resulting homogeneous areas of Sado Estuary are depicted in Figure 5.

TABLE 1. Statistics Regarding the Number and Area of Patches Produced by the Four Classification Approaches[a]

groups	OM (%)	%FF (%)	E_h (%)	total area (%)	no. of areas	min area (km^2)	max area (km^2)
			Method 1				
1, HO	8.6 ± 2.4	60.4 ± 27.0	−278.9 ± 68.6	9.48	19	0.0005150	1.06
2, MHO	4.2 ± 1.4	21.7 ± 11.8	−178.8 ± 72.6	38.24	26	0.0000110	9.13
3, MO	1.9 ± 0.7	9.1 ± 7.8	−137.4 ± 50.9	28.15	13	0.0014370	6.28
4, LO	0.9 ± 0.3	1.5 ± 1.3	74.4 ± 49.0	24.11	12	0.0000100	8.00
				total no, of areas	70		
				no. of areas ≤0.375 km^2	51		
			Method 1.1				
1, HO	7.6 ± 2.4	50.5 ± 25.7	−245.7 ± 80.3	11.70	15	0.0087419	1.45
2, MHO	2.9 ± 1.3	14.1 ± 9.3	−171.8 ± 56.0	65.12	11	0.0000008	35.96
3, Und	5.3 ± 1.6	34.0 ± 20.2	11.1 ± 53.7	0.28	4	0.0300000	0.05
4, LO	0.9 ± 0.4	1.7 ± 1.9	74.4 ± 48.4	22.91	8	0.0300000	7.49
				total no. of areas	38		
				no. of areas ≤0.375 km^2	28		
			Method 2				
1, HO	4.1 ± 0.9	23.2 ± 9.1	−237.9 ± 41.0	21.58	17	0.0000008	2.93
2, MHO	2.9 ± 0.4	13.0 ± 3.9	−152.1 ± 41.6	34.58	17	0.0005310	6.27
3, MO	1.9 ± 0.3	6.1 ± 2.4	−78.7 ± 52.3	28.15	7	0.0010410	13.68
4, LO	1.1 ± 0.2	1.5 ± 0.7	45.4 ± 47.1	15.71	7	0.0300000	6.66
				total no. of areas	48		
				no. of areas ≤0.375 km^2	29		
			Method 3				
1, HO		same as method 2		16.02	22	0.0000013	1.97
2, MHO		same as method 2		40.75	15	0.0008560	9.93
3, MO		same as method 2		25.98	15	0.0010410	11.20
4, LO		same as method 2		17.24	8	0.0100000	7.09
				total no. of areas	60		
				no. of areas ≤0.375 km^2	41		

[a] LO, low organic load; MO, medium organic load; MHO, medium high organic load; HO, high organic load; Und, Undefined.

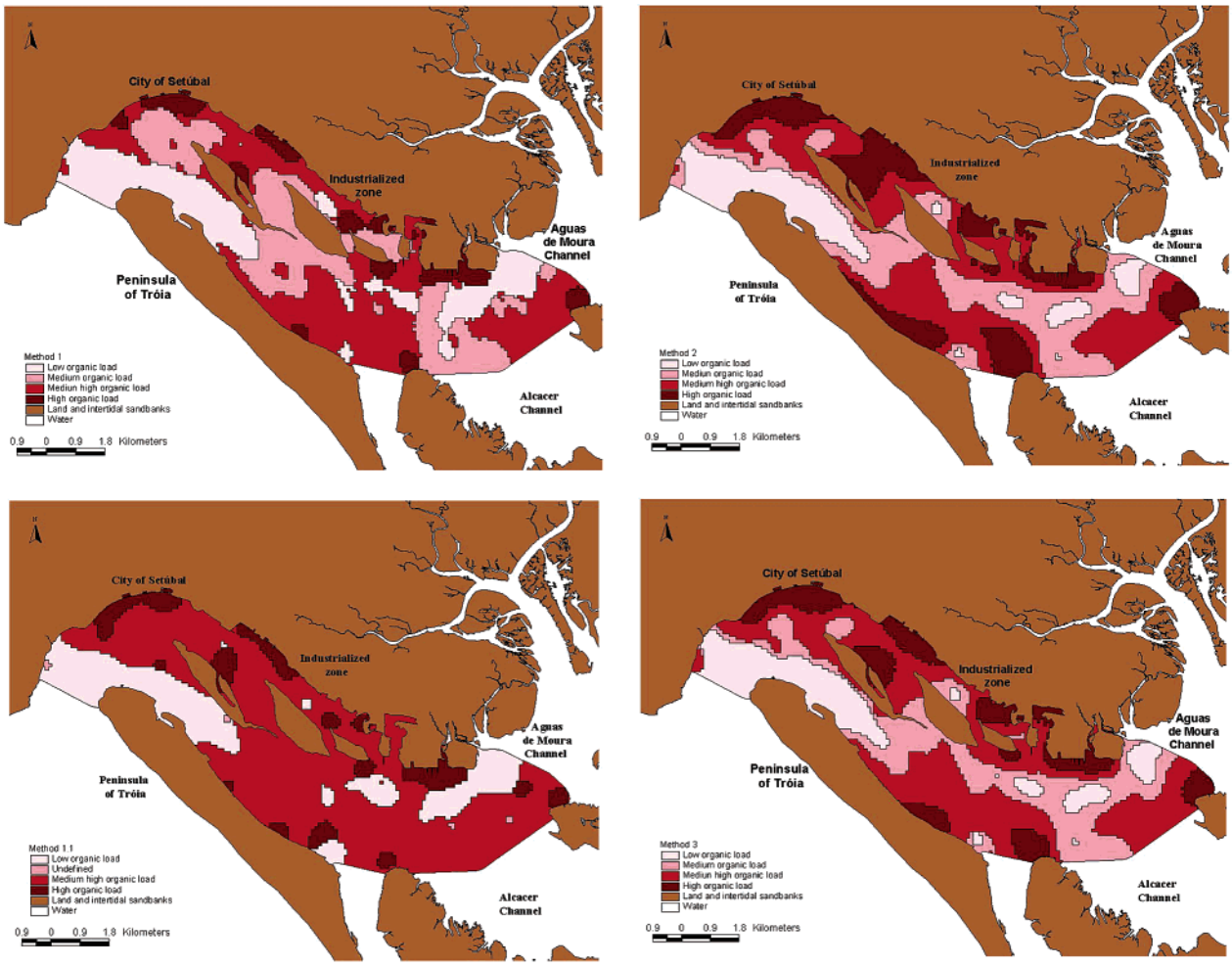

FIGURE 5. Homogeneous management areas for Sado Estuary generated by methods 1−3.

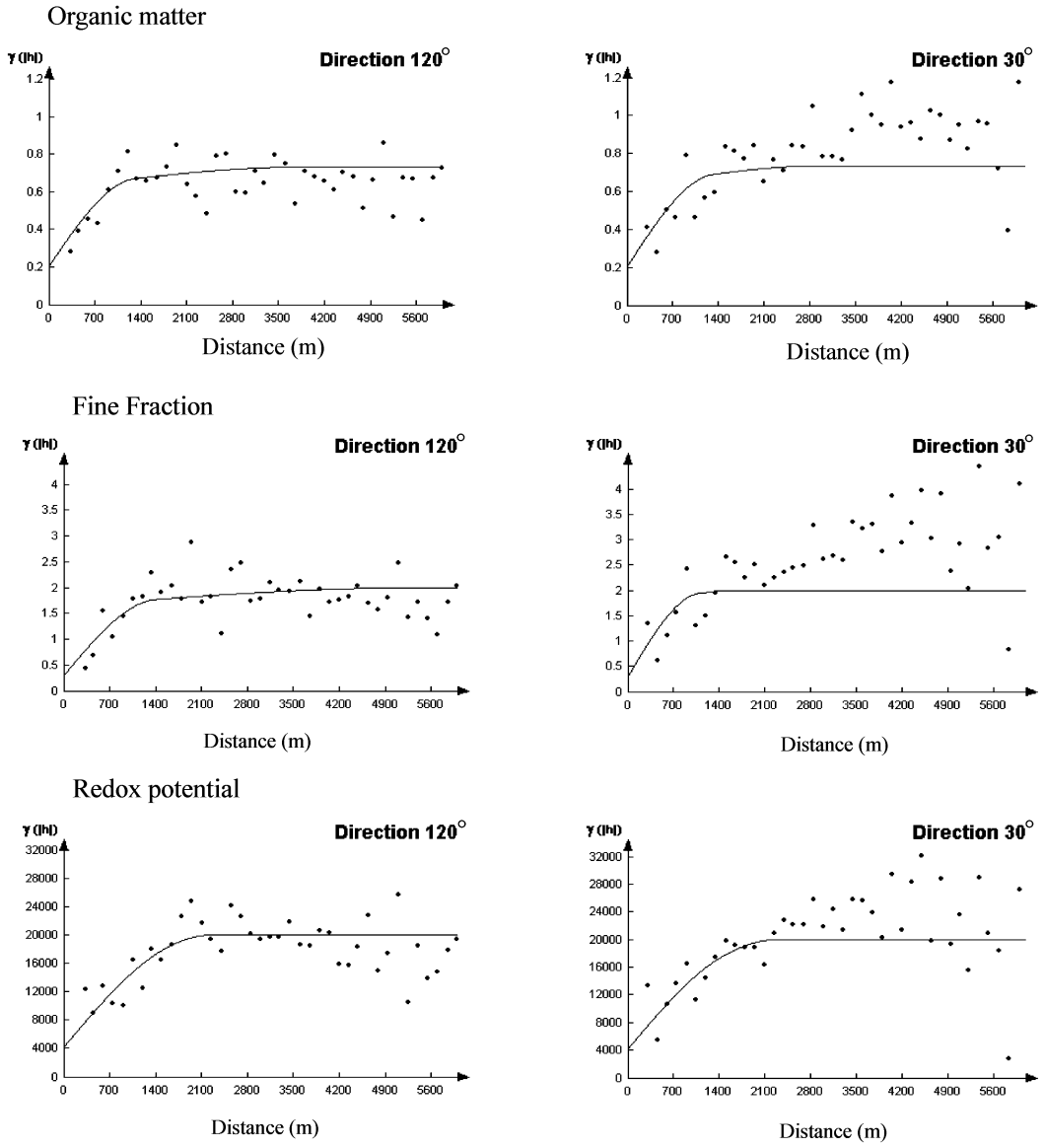

FIGURE 6. Experimental directional semivariograms and model fitted in the major and minor directions of anisotropy for the three attributes.

In method 3, the homogeneous areas were delineated by combining the previous two methodologies using eq 6 (Figure 5).

Despite some differences between methods 1−3 (see Table 1), their results generally are in agreement with earlier work performed in the estuary (*24*). Low organic load sediments correspond essentially to the estuarine entrance and tend to extend to the inside of the estuary, basically through the southern channel. This is confirmed in all method results by the presence, at the estuary entrance, of a large homogeneous area of low organic load (Figure 5). At the middle of the estuary bay, the gradient splits into two major components, one directed toward the North Channel and the other toward the South Channel. All methods indicate that in the estuary bay the class of medium high organic load is of largest extent (until 40% of the total area; Figure 5 and Table 1). Since high organic load areas are associated with low hydrodynamics and rich organic discharges, they are more common in the North Channel near industrialized zones and the city of Setubal. They are also distributed in small homogeneous areas (Figure 5). In methods 1 and 3, those areas are the less important in the estuary bay, representing respectively 9.48 and 16.02% of the total study area (Table 1), while the proportion is 21.58% for method 2 (Figure 5 and Table 1). According to historical and expert knowledge of the estuary, this last proportion is an overestimation of this type of sediment. However, special care must be taken when comparing high organic load clusters for methods 1 and 2 and method 3. High organic load cluster of methods 2 and 3 displays smaller values for OM and FF and higher values of E_h. Method 2 produced a smaller total number of areas (48 as compared to 70 and 60 in methods 1 and 3, respectively) and fewer areas smaller than the grid cell size (Table 1).

Stratifications produced by methods 2 and 3 share similar spatial patterns (Figure 5). Analysis of the κ values shows almost perfect agreement between maps 2 and 3 ($\kappa = 0.85$) (*25*). This result might be due to method 3 being a refinement of the discriminant analysis applied in method 2 using the local probabilities estimated with indicator kriging in method 1. The main differences reside in smaller areas of high organic load and larger areas with medium high organic load in method 3 (Table 1 and Figure 5). The spatial contiguity of the interpolated clusters of method 2 combined with the high density and systematic sampling of sediment can explain the lack of benefit of using the indicator kriging probabilities in method 3.

Method 3 is moderately similar to method 1 ($\kappa = 0.55$). These maps are created using different multivariate geo-

statistics, but method 3 uses results from method 1.

Methods 1 and 2 are the ones with less agreement (κ = 0.42) since the computed management areas use independent interpolation techniques (*25*).

The higher number of areas smaller than the sampling grid size (see Table 1) is also due to the clip with the study area boundary and should be ignored for delineation of estuarine management areas. It was only considered important in this paper for the original methods comparison. In further developments of this large project of estuarine management, areas smaller than the sampling grid size are assigned to the neighboring area that shares the longest common boundary (*26*).

In conclusion, after discarding the smallest areas, all methods will yield 19 management areas (Table 1) that are fairly contiguous and reproduce well the estuary environment. Also the κ values indicate that the maps are similar according to Landis and Koch (*27*) classification, supporting the choice of any of the methods as appropriate for management of the Sado Estuary. Nevertheless method 1 seems to be in better agreement with estuary behavior and earlier work conducted in the estuary in terms of estuary hydrodynamics (*15*), spatial distribution of sediment structure and benthic faunal assemblages (*24*), and identification of areas of contaminant sources. In summary, method 1 shows a more realistic pattern and detection of focal areas important for cost-effective management and thus long-term monitoring.

Acknowledgments

We thank the Sado Estuary Natural Reserve for providing the logistics, including boat and personnel support, during the sampling campaign. Comments by two anonymous reviewers also improved the presentation of this paper. Most of the work was accomplished during S.C.'s visit to the University of Michigan, which was supported by the Luso-American Foundation for Development (FLAD) and a PRODEP scholarship. The research was approved by the Portuguese Science and Technology Foundation and POCTI (Research Project POCTI/BSE 35137/99) and financed by FEDER.

Supporting Information Available

Additional information including 5 tables and 1 figure. This material is available free of charge via the Internet at http://pubs.acs.org.

Literature Cited

(1) Caeiro, S.; Painho M.; Costa, M. H.; Ramos, T. B. *Proceedings of International Conference on Sustainable Management of Coastal Ecosystems*; Duarte, P., Ed.; Fernando Pessoa University Press: Porto, 2002; pp 101−112.

(2) Kitsiou, D.; Tsirtsis, G.; Karydis, M. *Environ. Monit. Assess.* **2001**, *7* (1), 1−12.

(3) Jacquez, G. M.; Maruca, S.; Fortin, M. J. *J. Geogr. Syst.* **2000**, *2*, 221−241.

(4) Soares, A. *Geostatística para as Ciências da Terra e do Ambiente*; IST Press: Lisbon, 2000.

(5) Wackernagel, H. *Multivariate Geostatistics*: *An Introduction with Applications*; Springer-Verlag: Berlin, 1995.

(6) Oliver, M. A.; Webster, R. A. *Math. Geol.* **1989**, *21* (1), 15−35.

(7) Reed, J.; Chappel, A.; French, J. R.; Oliver, M. A. *Proceeding of GeoENV 2000−Geostatistics for Environmental Applications*, Avignon, 2000; pp 1−13.

(8) Goovaerts, P. *J. Geogr. Syst.* **2002**, *4*, 99−111.

(9) Goovaerts, P. *Geostatistics for Natural Resources Evaluation*; Oxford University Press: New York, 1997.

(10) Barabás, N.; Goovaerts, P.; Adriaens, P. *Environ. Sci. Technol.* **2001**, *35* (16), 3294−3301.

(11) Costa, F. O.; Correia, A. D.; Costa, M. H. *Ecotoxicol. Environ. Saf.* **1998**, *40*, 81−87.

(12) Cerejeira, M. J.; Pereira, T.; Espirito-Santo, J.; Viana, P.; Brito, F.; Morbey, M. *Proceedings of the 6th Conferência Nacional sobre a Qualidade do Ambiente*; Santana, F., Vasconcelos, L., Partidáro, M. R., Seixas, M. J., Sobral, M. P., Eds.; New University of Lisbon: Lisbon, 1999; Vol. 2, pp 133−142.

(13) Caeiro, S.; Goovaerts, P.; Painho, M.; Costa, M. H.; Sousa, S. *J. Environ. Model.* (in press).

(14) Flatman, G. T.; Englund, E. J.; Yfantis, A. A. *Principles of Environmental Sampling*; Keith, L. H., Ed.; ACS Professional Reference Book; American Chemical Society: Washington, DC, 1987; pp 73−92.

(15) Martins, F.; Leitão, P.; Silva, A.; Neves, R. *Oceanol. Acta* **2001**, *24*, S51−S62.

(16) Gibson, G. R.; Bowman, M. L.; Gerritsen, J.; Snyder, B. D. *Estuarine and Coastal Marine Waters: Bioassessment and Biocriteria Technical Guidance*; EPA 822-B-00-024; U.S. Environmental Protection Agency, Office of Water: Washington, DC, 2000.

(17) Engle, V.; Summers, J. K. *Environ. Monit. Assess.* **1998**, *51*, 381−397.

(18) Buchanan J. B. *Methods for the Study of Marine Benthos*; Holmes, N. A., McIntyre, A. D., Eds.; Blackwell Scientific Publication: Oxford, 1984.

(19) Little, L. S.; Edwards, D.; Porter, D. E. *J. Exp. Mar. Biol. Ecol.* **1997**, *213*, 1−11.

(20) Everitt, B.; Dunn, G. *Applied Multivariate Data Analysis*; Arnold Publishers and Oxford University Press: London, 2001.

(21) Bierkens, M. F. P.; Burrough, P. A. In *Geostatistics Troia 92*; Soares, A., Ed.; Kluwer Academic Publishers: Dordrecht, 1993; Vol. 2, pp 637−648.

(22) Cohen, J. *Educ. Psychol. Meas.* **1960**, *20*, 37−46.

(23) Goovaerts, P.; Webster, R. *Eur. J. Soil Sci.* **1994**, *45*, 79−95.

(24) Rodrigues, A. M.; Quintino, V. M. S. *Neth. J. Aquat. Ecol.* **1993**, *27* (2−4), 449−464.

(25) Sousa, S.; Caeiro, S.; Painho, M. *Proceedings of ESIG 2002*, Oeiras, 2002; pp 1−6.

(26) Caeiro, S.; Nunes, L.; Goovaerts, P.; Costa, H.; Cunha, M. C.; Painho, M.; Ribeiro, L. In *geoENV IV−Geostatistical for Environmental Applications*; Soares, A., Gomez-Hernandez, J., Froidevaux, R., Eds.; Kluwer Academic Press: Dordrecht (in press).

(27) Landis, J. R.; Koch, G. G. *Biometrics* **1977**, *33*, 159−174.

Received for review October 3, 2002. Revised manuscript received May 1, 2003. Accepted May 12, 2003.

ES0262075